Energy Dependence of the $^{51}V(p,n)^{51}Cr$ Analog Transition Between 16 and 26 MeV*

C. Wong, J. D. Anderson, J. C. Davis, and S. M. Grimes
Lawrence Livermore Laboratory, Livermore, California 94550
(Received 18 December 1972)

Utilizing the recently completed cyclograaff facility, we have measured the angular distribution of the $^{51}V(p,n)^{51}Cr$ analog transition between 16 and 26 MeV. Between 21 and 26 MeV the integrated cross section decreases monotonically with increasing energy while between 16 and 21 MeV a broad resonant behavior is observed. Coupled-channel calculations, with isospin strengths linearly scaled up 1.5% per MeV from the optimum values deduced at 26 MeV, provide a good description of the measurements between 21 and 26 MeV. However, in the region of the apparent resonance the measurements are systematically higher than the calculations at the backward angles, implying a correlation between the appearance of the broad structure and the increase of cross section at the backward angles. Similarly, search routines on the isospin strengths produced a significant improvement in the fits only between 21 and 26 MeV. Between 21 and 16 MeV, the isospin strengths increase to account for the increasing total cross section but the quality of the fits is essentially unchanged. Thus, the most likely explanation for the resonant behavior is not an energy dependence of the isospin strengths, but the presence of an additional reaction mechanism which yields either an isotropic or symmetric incoherent contribution to the (p,n) analog transition.

INTRODUCTION

In a previous paper[1] we reported measurements of quasielastic (p, n) scattering between 17 and 19 MeV on a number of medium-weight nuclei utilizing the Livermore variable-energy 90-in. cyclotron. Coupled-channel calculations, using a complex isospin interaction inferred from Becchetti and Greenlees[2] (BG) global optical potentials, yielded a good over-all average description of the measurements although discrepancies were observed for ^{51}V, ^{48}Ti, and ^{45}Sc at the backward angles. Comparison of calculations with measurements of Batty *et al.*[3] at 30 and 50 MeV showed that the isospin strengths did not change between 18 and 30 MeV and decreased by 30% between 30 and 50 MeV. In retrospect, these latter conclusions should be regarded as tentative and qualitative since the measurements of Batty *et al.* were limited to the forward angles ($\theta \leq 60°$) and were not complete enough to infer quantative estimates of the energy dependence of the isospin strengths. Indeed, recent measurements by the University of California at Los Angeles (UCLA) group[4] of the total quasielastic (p, n) cross section using $\tilde{p}$ decay showed that the isospin strengths are also decreasing between 18 and 30 MeV. Even assuming a reasonable energy dependence for the isospin strengths, the UCLA group was unable to explain their measurements which showed a broad resonant behavior, i.e., a rise and fall in the total quasielastic (p, n) cross section about 5 MeV above threshold. With the completion of the cyclograaff facility, it was thought worthwhile to investigate the $^{51}V(p, n)^{51}Cr$ quasielastic transition as a function of energy. Hopefully, angular distribution measurements between 16 and 26 MeV might not only determine the energy dependence of the isospin strengths in this energy region, but also yield further information on the anomalous behavior of the total (p, n) quasielastic cross section 5 to 10 MeV above threshold.

EXPERIMENTAL METHOD

The experimental method is described in Ref. 1. The ^{51}V target was a self-supporting metal foil of thickness 7.9 mg/cm^2. 10 collimated 10.8-m flight paths with 10 NE 213 detectors were employed for simultaneous data acquisition; the laboratory angles of observation were 3.5, 24, 39, 54, 69, 83, 99, 113, 129, and 144°. To increase the flight time available for observation of the neutrons, the 15-MeV cyclotron beam was passed through rf sweeper plates which reduced the beam frequency from 25 to 5 MHz. The beam then enters an EN tandem Van de Graaff for acceleration to its final energy. In order to prevent overlap of the low-energy neutrons with high-energy neutrons from a later cycle, neutron detector biases of 3.5 and 5.4 MeV were employed. The 5.4-MeV bias was utilized above a bombarding energy of 17 MeV. These biases are also sufficiently high to prevent the detection of $^{12}C(n, 3\alpha)$ events in the NE 213 scintillators for the quasielastic neutron group, thereby allowing us to use a calculated efficiency based on np scattering alone. The 3.5-MeV neutron bias corresponded in pulse height with the Compton edge of the 1.28-MeV γ ray from a ^{22}Na source and is denoted as "high ^{22}Na bias." 5.4-MeV neutron bias corresponded to a pulse-height setting of twice "high ^{22}Na bias." The conversion from electron to equiv-

TABLE I. Fraction of recoil pulses above bias calculated for three incident neutron energies assuming isotropic and anisotropic *np* scattering.

E_n (MeV)	Bias [a] (MeV)	Isotropic	Anisotropic
10	3.5	0.650	0.656
10	5.5	0.450	0.457
20	3.0	0.850	0.853
20	5.5	0.725	0.731
30	3.75	0.875	0.872
30	6.0	0.800	0.798

[a] Bias settings are approximately those employed in the present measurements.

alent recoil proton bias settings for NE 213 was obtained using the measurements of Pohl *et al.*[5] The efficiency was calculated assuming that carbon elastic scattering did not attenuate the neutron beam:

$$\epsilon = (1 - e^{-(\sigma_H N_H + \sigma_{n\epsilon} N_C)L}) \frac{\sigma_H N_H}{\sigma_H N_H + \sigma_{n\epsilon} N_C} \frac{E_n - E_B}{E_n}, \quad (1)$$

where L is the length of the cylindrical 5.08-cm $\times$5.08-cm scintillator, σ_H the total *np* cross section, $\sigma_{n\epsilon}$ the carbon nonelastic cross section, N_H and N_C are, respectively, the number of hydrogen and carbon atoms per cm^3, E_n is the neutron energy, and E_B is the bias energy. Another calculation was made in which the efficiency included the primary hydrogen collisions and carbon-hydrogen collisions. It was assumed that the carbon scattering was isotropic and that the carbon total cross section was all elastic. With these extreme assumptions, the two efficiency calculations differed by at most 5% over the neutron energy range up to 30 MeV. From these comparisons and also previous comparisons between calculated and measured efficiencies for a 2.54-cm$\times$2.54-cm plastic scintillator it is estimated that the efficiency calculated with Eq. (1) [excluding the $(E_n - E_B)/E_n$ factor] should be good to ±7%.

The factor $(E_n - E_B)/E_n$ implies that *np* scattering is isotropic in the c.m. system. Since *np* scattering is not exactly isotropic, we have computed the fraction of the recoil pulses counted at a detector bias E_B assuming isotropy and assuming the anisotropic angular distributions calculated by Hopkins and Breit[6] employing the Yale phase shifts. The results are given in Table I which shows that the maximum error assuming isotropy is 1.5% and occurs for 10-MeV neutrons at ~5.4-MeV bias. Since this error is much smaller than the above estimated ±7% uncertainty in the efficiency calculation, the fraction of recoil pulses

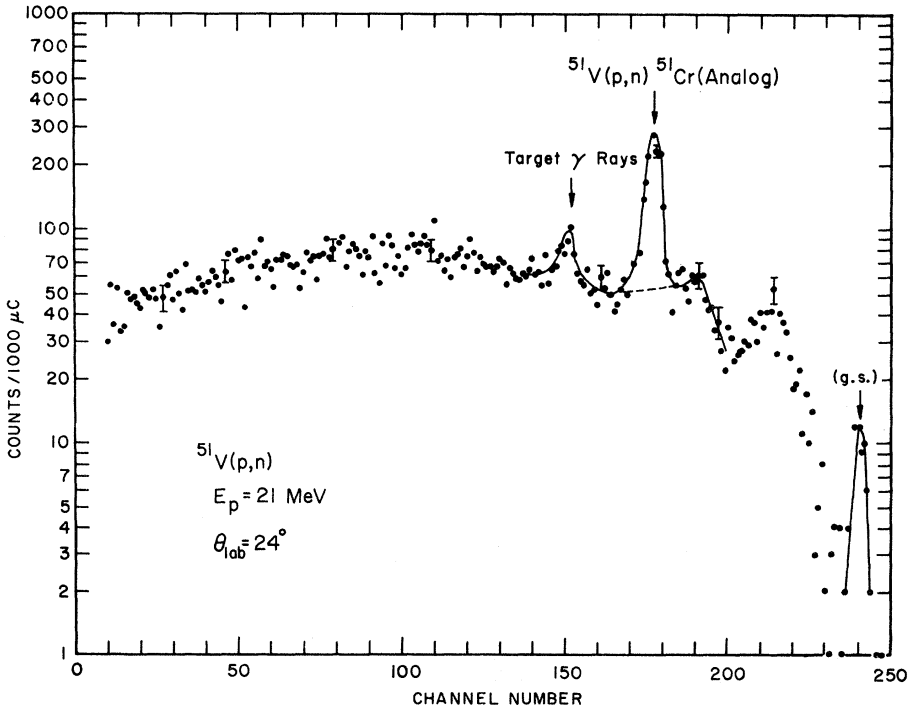

FIG. 1. Typical time-of-flight neutron spectrum from $^{51}V + p$. The bombarding energy was 21 MeV and the angle of observation was 24°. Time calibration of the system was 0.64 nsec/channel. Increasing time-of-flight is toward the left.

detected was computed with the expression $(E_n - E_B)/E_n$.

EXPERIMENTAL RESULTS

A typical time-of-flight spectrum is shown in Fig. 1. Evident are the analog state neutron group and the neutron continuum from compound, pre-equilibrium, and other emission processes. The neutron continuum beneath the analog state neutron group was estimated by means of the dashed curve in Fig. 1. The errors on the quasielastic cross sections include not only counting statistics, but also the uncertainties involved in estimating the continuum background beneath the quasielastic neutron peak. This background uncertainty contributes negligible error at the forward angles, where the quasielastic peak is prominent and most of the error at the backward angles, where the quasielastic cross section is small. However, the error in the quasielastic cross sections is in no case less than 7%, which represents an estimate of the absolute accuracy of the efficiency calculation. The measured angular distributions as a function of bombarding energy are displayed in Fig. 2. Data at 19 MeV and some data at 20 MeV are missing because of the overlap of the quasielastic neutron group with target γ rays from a later cycle. Although proton-electron pulse-shape discrimination was employed, the suppression of γ rays was not 100% effective.

The angular distributions were fitted with a Legendre-polynomial expansion; usually a seven-term expansion provided a reasonable fit to the data. From the zero-order coefficient, the integrated cross sections were obtained and are plotted as dots in Fig. 3. The squares were obtained from a Legendre-polynomial fit to previously published[1] ^{51}V data, which were taken on the 90-in. cyclotron using plastic scintillators. Inspection of Fig. 3 reveals reasonable agreement between cyclograaff measurements taken with NE 213 scintillators and 90-in. cyclotron measurements taken with plastic scintillators.

CALCULATIONS

As described in Ref. 1, the quasielastic differential cross sections were calculated for ^{51}V between 16 and 26 MeV using a coupled-channel code. An isospin-dependent optical potential was employed whose parameters were deduced from the BG global fits to proton and neutron elastic scattering and polarization data. Figure 2 shows some of these calculations for ^{51}V at 18, 21, and 26 MeV (see solid lines). At 18 MeV the calculations are lower than the measurements at the backward angles, in agreement with the results presented

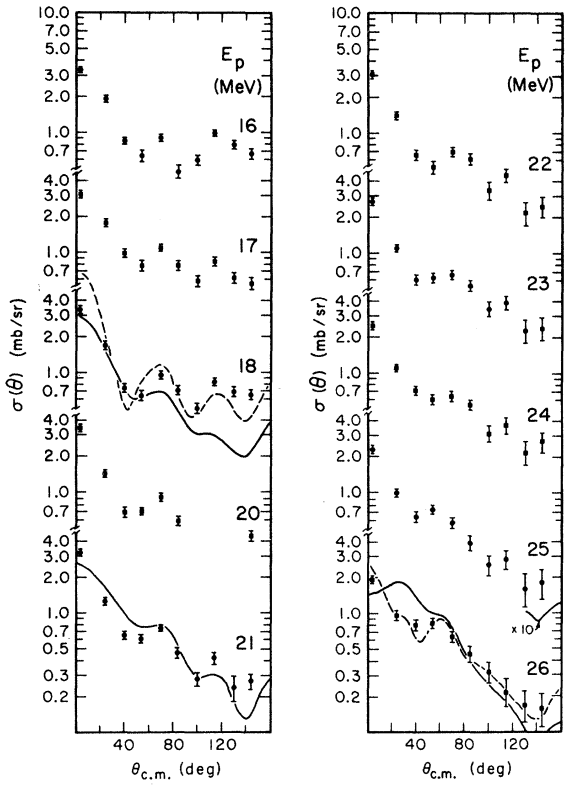

FIG. 2. The $^{51}V(p,n)^{51}Cr$ analog state angular distribution as a function of bombarding energy. The solid lines are the angular distributions calculated employing parameters deduced from the BG global fits to neutron and proton elastic scattering and polarization data. Dashed curves are optimum fits obtained by varying V_{1V} and V_{1S} with $W_{1S}=36$ MeV (see Table III).

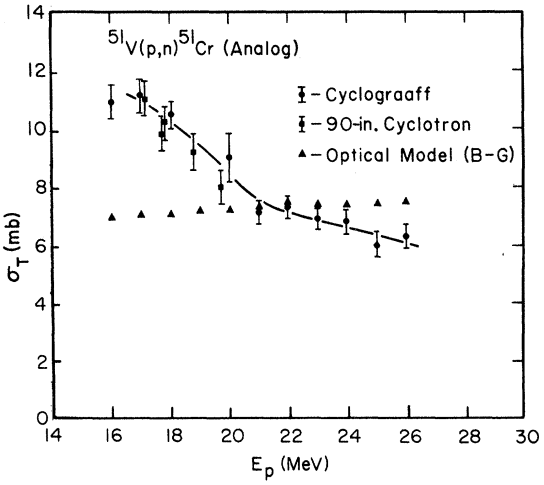

FIG. 3. The $^{51}V(p,n)^{51}Cr$ analog state integrated cross sections as a function of bombarding energy. See text for significance of the various symbols. The dashed curve is merely a smooth curve through the cyclograaff and 90-in. cyclotron measurements.

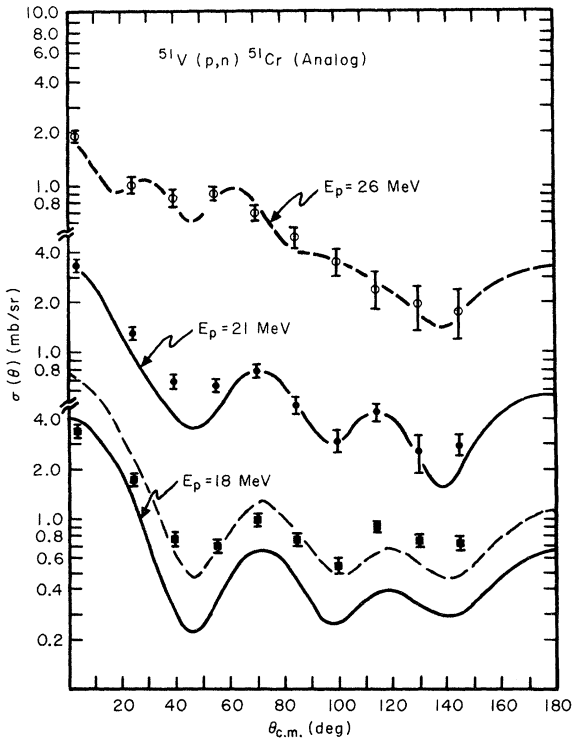

FIG. 4. Solid lines are coupled-channel calculations of the quasielastic angular distributions with isospin strengths at 21 and 18 MeV linearly scaled up 1.5% per MeV from the optimum strengths deduced at 26 MeV. Dashed curves are optimum fits at 26 and 18 MeV obtained by searching on V_{1V} and W_{1S} with $V_{1S}=0$ (see Table II for optimum strengths).

for ^{51}V in Ref. 1 between 17 and 19 MeV. At 21 MeV there is reasonable agreement while at 26 MeV the angular distribution at the forward angles is poorly described by the calculations. The integrated cross sections from the coupled-channel calculations are displayed as triangles in Fig. 3. It is immediately obvious that the major discrepancy between measurements and calculations occurs in the region between 16 and 20 MeV. There is an apparent correlation between the appearance of the broad maximum in the integrated cross section and the increase of cross section at the backward angles.

To improve the fit at 26 MeV, a search routine was instituted on the isospin strengths V_{1V} and W_{1S}, where V_{1V} is the volume real isospin strength and W_{1S} is the surface imaginary isospin strength. Starting with BG values[7] of $V_{1V}=96$ MeV, $W_{1S}=48$ MeV, and a χ^2 value of 33.7, an optimum fit with $\chi^2=2.7$ was obtained for $V_{1V}=37$ MeV and $W_{1S}=82$ MeV. This optimum fit at 26 MeV is displayed in Fig. 4. The isospin strengths at 26 MeV were then scaled up 1.5% per MeV with decreasing energy and the angular distributions calculated at 21 and 18 MeV. The results of these latter calculations are also shown as solid lines in Fig. 4. The disagreement at 18 MeV at the backward angles still persists in spite of the fact that reasonable agreement is now obtained at 21 MeV.

Search routines on the isospin strengths were instituted to see if the resonant behavior could be accounted for by an energy dependence of the isospin strengths. Table II shows the results at 18 and 26 MeV searching on V_{1V} and W_{1S} with the real surface strength (V_{1S}) set equal to zero. These optimum fits are also displayed as dashed curves in Fig. 4. At 26 MeV the fit is significantly improved, i.e., χ^2 is reduced by over an order of magnitude below the BG value, while at 18 MeV the total cross section is in reasonable agreement but the quality of fit is not greatly improved (see Table II and Fig. 4).

Table III shows the results searching on V_{1V} and V_{1S} holding $W_{1S}=36$ MeV. The optimum fits corresponding to the final searched values of Table III are shown as dashed curves in Fig. 2. As in Table II and Fig. 4, Table III and Fig. 2 show that at 18 MeV the shape of the angular distribution is not fitted well by varying the isospin strengths. A third search was instituted on V_{1S} and W_{1S} holding $V_{1V}=40$ MeV. Because V_{1S} and W_{1S} had the same radial form factor, the search routine did not give unique separate values for V_{1S} and W_{1S}. Several combinations of V_{1S} and W_{1S} values gave similar χ^2 results. Again, this search showed that the χ^2 value is significantly improved only for the 26-MeV data.

Although the BG potential and those used in the search routines do not rigorously conserve isospin,[8] the effect of this violation on the calculated

TABLE II. V_{1V}, W_{1S}, σ_T, and χ^2 values at 18 and 26 MeV corresponding to the optimum fits shown as dashed curves in Fig. 4.

			Final searched values ($V_{1S}=0$)			
E_p	σ_T (measured) (mb)	χ^2(BG)	V_{1V}	W_{1S}	σ_T	χ^2
18	10.5 ± 0.7	42.2	69.5	118.6	11.5	11
26	6.3 ± 0.4	33.7	37	82	6.2	2.7

TABLE III. V_{1V}, V_{1S}, σ_T, and χ^2 values at 18 and 26 MeV corresponding to the optimum fits shown as dashed curves in Fig. 2.

			Final searched values ($W_{1S}=36$ MeV)			
E_p	σ_T (measured) (mb)	χ^2(BG)	V_{1V}	V_{1S}	σ_T	χ^2
18	10.5 ± 0.7	42.2	38.1	105.4	11.1	14.8
26	6.3 ± 0.4	33.7	36.7	54.7	6.2	3.2

(p,n) cross section is, in general, small. The (p,n) cross section is dependent upon only the strength and form factor of the isospin interaction and the optical absorption. However, for some extreme cases (i.e., predominantly surface imaginary coupling) the above weak-coupled scaling[9,10] does not apply, and the proton elastic scattering is significantly modified.[8] It should be emphasized that our parameters do not rigorously conserve isospin; hence the differences between proton and neutron potentials are inconsistent with our quoted real and imaginary isospin strengths. However, these discrepancies should not be viewed as significant evidence implying isospin nonconservation, since they may well result from ambiguities in neutron potentials caused by the paucity of accurate neutron elastic scattering and polarization data.

CONCLUSION

Between 21 and 26 MeV, the shape and magnitude of the angular distributions can be fitted well by searching on the isospin strengths. At 18 MeV no such improvement is possible: the search routine yields closely the correct total cross section, but the shape at forward and backward angle is poorly fitted. In particular, the calculations cannot simultaneously fit the forward and backward angle data. These results suggest that the direct quasielastic (p,n) reaction model cannot account for the angular distributions around 18 MeV; the measured cross sections are invariably higher than the calculations at the backward angles.

The most likely explanation is the presence of a contribution from another reaction mechanism which produces an angular distribution much more isotropic than that from a one-stage direct process. Such possible mechanisms are (a) three-stage direct processes, (b) equilibrium decay of overlapping analog states in the compound system, (c) neutron decay from analog giant resonances ($E1$ or $E2$), and (d) pre-equilibrium decay of compound analog states. Contributions from mechanism (a) would result from sequential (p,p'), then charge exchange followed by (n',n). The absence of (p,n) groups corresponding to excited analogs argues against three-stage as well as two-stage direct processes.

The cross section for equilibrium reactions through analog states in the compound system is $1/(2T+1)$ times the reaction cross section.[11] The magnitude of this quantity, assuming a reaction cross section of 1 b, is 160 mb. Only a small fraction of this flux would be needed to explain the observed anomaly. However, the energy dependence predicted for such a mechanism would be a rapid rise beyond threshold and an exponential drop beyond the peak. For typical nuclear temperatures in this mass region, the decrease would be about a factor of 3 per MeV, an energy dependence contradicted by the data.

Somewhat more tentative conclusions characterize the remaining possibilities. The position of the $T^>E1$ giant resonance in ^{52}Cr may be estimated by adding the isospin splitting energy to the $T^<E1$ resonance energy. A value for the splitting of 2.3 MeV was obtained from Akyüz and Fallieros[12] and was added to the energy[13] of the $T^<$ resonance of 19 MeV, yielding the value 21.3 MeV for the analog $E1$ resonance in ^{52}Cr. This is much lower than our observed excitation energy of 26.5 MeV (bombarding energy $\approx$ 16 MeV). Moreover, the use of a single-level Breit-Wigner formula yields an estimate for Γ_p which is at least an order of magnitude larger than that measured for the ^{88}Sr and ^{90}Zr systems by Hasinoff *et al.*[14] While the A dependence of Γ_p is not too well known, a variation of an order of magnitude would not be expected.

An estimate of 16 MeV for the excitation energy of the $E2$ $T^<$ resonance in this mass region may be obtained from the $^{51}V(p,p')$ measurements of Tyren and Maris[15]; making the assumption that the isospin splitting is equal to that for the $E1$ resonances, we obtain a value of 18.3 MeV for the excitation energy of the $E2$ $T^>$ giant resonance. Again, this position does not agree with the peak in our measured excitation function.

The most promising explanation is probably pre-equilibrium decay of $T^>$ states in the composite system. As was pointed out previously, a reaction cross section of 160 mb proceeds through $T^>$ states in the composite system. Quantitative calculations cannot be made without assuming values for the width of the intermediate states. If, however, it is assumed that the observed 4-mb enhancement of the cross section corresponds to pre-equilibrium decays of the first-formed three-exciton states, a total width of about 200 keV would be required for these states in order to produce the observed cross section. This value is based on a calculation of the proton width with the relation $P = 2\pi\Gamma_p^>/D_3^> = 1/(2T+1)$ and the neutron width with the equation $2T\Gamma_p^> = \Gamma_n$, as is predicted by isospin symmetry. The density of three-exciton states was calculated with a formula due to Ericson.[16] Using Griffin's[17] exciton model to calculate the expected energy dependence of the cross section yields an energy variation intermediate between the roughly constant cross section expected for a direct process and the exponential variation obtained for an equilibrium reaction. Although the fit to the data is better than that for either of these extremes, no quantitative agreement could be obtained.

*Work performed under the auspices of the U. S. Atomic Energy Commission.

[1]C. Wong, J. D. Anderson, J. W. McClure, B. A. Pohl, and J. J. Wesolowski, Phys. Rev. C **5**, 158 (1972).
[2]F. D. Becchetti, Jr., and G. W. Greenlees, Phys. Rev. **182**, 1190 (1969).
[3]C. J. Batty *et al.*, Nucl. Phys. **A116**, 643 (1968).
[4]G. W. Hoffmann, W. H. Dunlop, G. J. Igo, J. G. Kulleck, C. A. Whitten, Jr., and W. R. Coker, to be published.
[5]B. A. Pohl *et al.*, Lawrence Livermore Laboratory Report No. UCRL-50653, 1969 (unpublished).
[6]J. C. Hopkins and G. Breit, Nucl. Data **A9**, 137 (1971).
[7]The diagonal matrix elements of the isospin potential $(U_1/A)t\cdot\tau$ yield $\pm(U_1/4A)(N-Z)$, (+) for neutron elastic scattering and (−) for proton elastic scattering. Hence the B-G parametrization implies U_1 (volume real) $\equiv V_{1V}=96$ MeV and U_1 (surface imaginary) $\equiv W_{1S}=48$ MeV. The isospin volume form factor for V_{1V} is Woods-Saxon with radius and diffuseness identical to that given by BG for the volume real potential. The isospin surface form factors for V_{1S} and W_{1S} are derivative Woods-Saxon with radius and diffuseness identical to that given by BG for the surface imaginary potential.
[8]S. Cotanch and D. Robson, Phys. Rev. C (to be published).
[9]E. H. Schwarcz, Phys. Rev. **149**, 752 (1966).
[10]J. D. Anderson *et al.*, Phys. Rev. **177**, 1416 (1969).
[11]S. Grimes, J. D. Anderson, A. Kerman, and C. Wong, Phys. Rev. C **5**, 85 (1972).
[12]R. Ö. Akyüz and S. Fallieros, Phys. Rev. Lett. **27**, 1016 (1971).
[13]B. L. Berman, *Nuclear Spectroscopy II* (Academic, New York, to be published), Chap. IXA.
[14]M. Hasinoff, G. A. Fisher, H. M. Kuan, and S. S. Hanna, Phys. Lett. **30B**, 337 (1969).
[15]H. Tyren and Th. A. J. Maris, Nucl. Phys. **7**, 24 (1958).
[16]T. Ericson, Adv. Phys. **9**, 425 (1960).
[17]J. J. Griffin, Phys. Rev. Lett. **17**, 478 (1966).

PHYSICAL REVIEW C VOLUME 7, NUMBER 5 MAY 1973

Electric Dipole Strength in ^{23}Na Observed with the Capture Reaction ^{22}Ne$(p, \gamma_0+\gamma_1)^{23}$Na†

E. Ventura
Department of Physics, Stanford University, Stanford, California 94305
(Received 10 July 1972)

The differential cross section for the capture reaction ^{22}Ne$(p, \gamma_0+\gamma_1)^{23}$Na has been measured. Significant structure is observed in the giant-resonance region. Comparison with the reaction ^{23}Na$(\gamma, n)^{22}$Ne indicates a splitting of the dipole strength. Possible sources of this splitting are discussed.

I. INTRODUCTION

The study of giant dipole resonances in the deformed nuclei of the *s-d* shell are of particular interest in view of the various mechanisms that can contribute to split the dipole strength. Some of these are: (1) the Danos-Okamoto effect[1,2] that splits the giant resonance into two groups of transitions corresponding to dipole vibrations along the major and minor axes of the nuclear ellipsoid, (2) the isospin splitting into $T_<$ and $T_>$ groups,[3] and (3) configurational splitting[4,5] that divides the dipole strength into two groups: a lower group associated with transitions from the outer $2s$-$1d$ shell into the $2p$-$1f$ shell and a higher group associated with transitions from the inner $1p$ shell into the $2s$-$1d$ shell.

Most of the work in this mass region, both through direct and inverse photonuclear reactions, has concentrated on even-A nuclei, whereas few investigations have been performed on odd-A nuclei, and these mostly by photonuclear reactions. Therefore, we have investigated the capture reaction ^{22}Ne$(p, \gamma)^{23}$Na throughout the giant-resonance region of ^{23}Na.[6]

II. EXPERIMENTAL PROCEDURE

Proton beams were generated by the Stanford FN tandem Van de Graaff accelerator. The target consisted of a cylindrical gas cell 5 cm in diameter filled with ^{22}Ne gas 97% pure, at a pressure of $\frac{1}{3}$ atm. The beam passed along a diameter of the cell and entered and exited through windows made of Ta foil 2.5×10^{-3} cm thick. The beam was stopped 9 m behind the target in a shielded beam dump. γ rays were detected in the Stanford 24-cm × 24-cm NaI(Tl) spectrometer.[7] 35 cm of paraffin were placed between the detector and the target in order to reduce the fast-neutron background. Figure 1 shows a spectrum taken at E_p = 10 MeV. Transitions to the ground and first excited states in ^{23}Na are seen. Since these states are only 0.44 MeV apart they could not be resolved. The data were analyzed with a computer program which fits, by the method of least squares, the